arXiv:cond-mat/0404381v2 [cond-mat.stat-mech] 1 Oct 2004

Observable Signature of the Berezinskii-Kosterlitz-Thouless Transition in a Planar Lattice of Bose-Einstein Condensates

A. Trombettoni[1], A. Smerzi[2,3], and P. Sodano[4]

[1] *Istituto Nazionale per la Fisica della Materia and Dipartimento di Fisica, Universita' di Parma, parco Area delle Scienze 7A, I-43100 Parma, Italy*

[2] *Istituto Nazionale per la Fisica della Materia BEC-CRS and Dipartimento di Fisica, Universita' di Trento, I-38050 Povo, Italy*

[3] *Theoretical Division, Los Alamos National Laboratory, Los Alamos, NM 87545, USA*

[4] *Dipartimento di Fisica and Sezione I.N.F.N., Università di Perugia, Via A. Pascoli, I-06123 Perugia, Italy*

(February 2, 2008)

Abstract

We investigate the possibility that Bose-Einstein condensates (BECs), loaded on a $2D$ optical lattice, undergo - at finite temperature - a Berezinskii-Kosterlitz-Thouless (BKT) transition. We show that - in an experimentally attainable range of parameters - a planar lattice of BECs is described by the XY model at finite temperature. We demonstrate that the interference pattern of the expanding condensates provides the experimental signature of the BKT transition by showing that, near the critical temperature, the $\vec{k}=0$ component of the momentum distribution and the central peak of the atomic density profile sharply decrease. The finite-temperature transition for a $3D$ optical lattice is also discussed, and the analogies with superconducting Josephson junction networks are stressed through the text.

I. INTRODUCTION

Recent advances in the manipulation of cold atomic gases allow nowadays for storing Bose-Einstein condensates (BECs) in $1D$ [1–5], $2D$ [6] and $3D$ [7] optical lattices, opening a pathway for the experimental and theoretical analysis of finite temperature transitions in atomic systems. In a way similar to the spectacular realizations obtained with superconducting Josephson networks [8,9], arrays of BECs can provide new experimentally realizable systems on which to test well known paradigms of the statistical mechanics: our interest here is to evidence how to detect a finite-temperature defect-mediated transition in $2D$ optical lattice of BECs.

According to the well-known Mermin-Wagner theorem [10], two-dimensional systems with a continuous symmetry cannot sustain long-range order in the thermodynamic limit at finite temperature; however, a phase transition is still possible and it occurs via the unbinding of point defects like dislocations or vortices. Defect-mediated transitions are widely studied [10] since they provide crucial insights for a wide variety of experiments on thin films. The BKT transition is the paradigmatic example of a defect-mediated transition [10] which is exhibited by the two-dimensional XY model [11,12], describing 2-components spins on a two-dimensional lattice. In the low-temperature phase, characterized by the presence of bound vortex-antivortex pairs, the spatial correlations exhibit a power-law decay; above a critical temperature T_{BKT}, the decay is exponential and there is a proliferation of free vortices. The BKT transition has been observed in superconducting Josephson arrays [9] and its predictions are well verified in the measurements of the superfluid density in ^4He films [13].

In finite magnetic systems the BKT transition point is signaled by the drop to 0 of a suitably defined magnetization [14]; the existence of such a magnetization in finite systems does not contradict the Mermin-Wagner theorem, since the latter is valid only in the thermodynamic limit. In a large class of experimental situations, the finite size XY model predicts magnetization exponents in agreement with the measurements carried out for layered magnets with planar spin symmetry [15]. We shall show in the sequel that the Fourier transform at $\vec{k} = 0$ of the condensates wavefunction provide the analogous of this magnetization for atomic systems, which are naturally finite (since they are trapped by an harmonic potential).

In this paper we show that - at a critical temperature T_{BKT} lower than the temperature T_{BEC} at which condensation in each well occurs - $2D$ lattices of BECs may undergo a phase transition to a superfluid regime where the phases of the single-well condensates are coherently aligned allowing for the observation of a Berezinskii-Kosterlitz-Thouless (BKT) transition. We show in the following that the recently realized $2D$ optical lattice of Bose-Einstein condensates [6] may allow for the observation of a BKT transition in a finite bosonic system, since the thermodynamic properties of the bosonic lattice at finite temperature may be well described, in a suitable and experimentally attainable range of parameters, by the Hamiltonian of the XY model. It is easy to convince oneself that the transition we propose to observe is different from the quantum phase transition reported in [7], where the system is at $T = 0$ and the insulator phase (signaled by a reversible destruction of the phase coherence across the lattice) is reached varying the optical lattice parameters: at variance, here, we propose to fix the system parameters in the superfluid phase and increase the temperature T until the thermally induced vortex proliferation determines the BKT transition.

We shall also show that the experimental signature of the BKT transition in bosonic planar lattices is obtained by measuring, as a function of the temperature, the central peak of the interference pattern of the expanding condensates released from the trap when the confining potentials are switched off. In fact, the peak of the momentum distribution at $\vec{k} = 0$ may be regarded as the magnetization of a finite size $2D$ XY magnet, and, as shown in the following, it should exhibit a sharp decrease around T_{BKT}. As a consequence, also the central peak of the atomic density profile decreases around T_{BKT}, signaling the occurrence of the BKT transition.

The plan of the paper is the following: in Section II we discuss the Hamiltonian describing a $2D$ lattice of Bose-Einstein condensates at finite temperature and we show that - in a suitable range of parameters - the system is described by the XY Hamiltonian. In Section

III we show how the signature of the BKT transition may be evidenced in a bosonic planar lattice; there we shall also discuss interesting analogies with superconducting Josephson junction networks. Section IV is devoted to our concluding remarks. In Appendix A we report the details of a variational estimate of the coefficients of the Hamiltonian describing $1D$, $2D$ and $3D$ optical lattices, while Appendix B contains the analytical computation of the Fourier transform of a vortex on a lattice.

II. THE FINITE-TEMPERATURE HAMILTONIAN FOR THE SYSTEM

For $2D$ optical lattices, when the polarization vectors of the two standing wave laser fields are orthogonal, the resulting periodic potential for the atoms is

$$V_{opt}(\vec{r}) = V_0[\sin^2(kx) + \sin^2(ky)] \tag{1}$$

where $k = 2\pi/\lambda$ is the wavevector of the laser beams. The potential maximum of a single standing wave, $V_0 = sE_R$, may be controlled by changing the intensity of the optical lattice beams, and it is conveniently measured in units of the recoil energy $E_R = \hbar^2 k^2/2m$ (m is the atomic mass), while, typically, s can vary from 0 up to 30 (gravity is assumed to act along the z-axis).

Usually, superimposed to the optical potential, there is an harmonic magnetic potential

$$V_m(\vec{r}) = \frac{m}{2}[\omega_r^2(x^2 + y^2) + \omega_z^2 z^2], \tag{2}$$

where ω_z (ω_r) is the axial (radial) trapping frequency. The minima of the $2D$ periodic potential (1) are located at the points $\vec{j} = (j_1, j_2) \cdot \frac{\lambda}{2}$ with j_1 and j_2 integers, and the potential around the minima is $V_{opt} \approx \frac{m}{2}\tilde{\omega}_r^2[(x - \lambda j_1/2)^2 + (y - \lambda j_2/2)^2]$ with

$$\tilde{\omega}_r = \sqrt{2V_0 k^2/m} \tag{3}$$

providing the frequency of the wells. When $\tilde{\omega}_r \gg \omega_r, \omega_z$, the system realizes a square array of tubes, i.e. an array of harmonic traps elongated along the z-axis [6]. Although the axial dynamics is very interesting in its own right [16], in the following we analyze only the situation in which the axial degrees of freedom are frozen out, which is realizable if ω_z is sufficiently large. We also assume that the harmonic oscillator length of the magnetic potential $\sqrt{\hbar/m\omega_r}$ is larger than the size L (in lattice units) of the optical lattice in order to reduce density inhomogeneity effects and to allow for a safe control of finite size effects. In addition, when all the relevant energy scales are small compared to the excitation energies one can safely expand the field operator [17] as

$$\hat{\Psi}(\vec{r},t) = \sum_{\vec{j}} \hat{\psi}_{\vec{j}}(t)\Phi_{\vec{j}}(\vec{r}) \tag{4}$$

with $\Phi_{\vec{j}}(\vec{r})$ the Wannier wavefunction localized at the $\vec{j}$-th well (normalized to 1) and $\hat{N}_{\vec{j}} = \hat{\psi}^{\dagger}_{\vec{j}}\hat{\psi}_{\vec{j}}$ the bosonic number operator. Substituting the expansion in the full quantum Hamiltonian describing the bosonic system, leads to the Bose-Hubbard model [18,17]

$$\hat{H} = -K \sum_{<\vec{i},\vec{j}>} (\hat{\psi}^{\dagger}_{\vec{i}}\hat{\psi}_{\vec{j}} + h.c.) + \frac{U}{2}\sum_{\vec{j}} \hat{N}_{\vec{j}}(\hat{N}_{\vec{j}} - 1) \tag{5}$$

where $\sum_{<\vec{i},\vec{j}>}$ denotes a sum over nearest neighbours, $U = (4\pi\hbar^2 a/m)\int d\vec{r}\,\Phi^4_{\vec{j}}$ (a is the s-wave scattering length) and $K \simeq -\int d\vec{r}\,[\frac{\hbar^2}{2m}\vec{\nabla}\Phi_{\vec{i}}\cdot\vec{\nabla}\Phi_{\vec{j}} + \Phi_{\vec{i}}V_{ext}\Phi_{\vec{j}}]$.

Upon defining

$$J = 2KN_0 \tag{6}$$

(where N_0 is the average number of atoms per site), when $N_0 \gg 1$ and $J/N_0^2 \ll U$, the Bose-Hubbard model reduces to

$$\hat{H} = H_{XY} - \frac{U}{2}\sum_{\vec{j}} \frac{\partial^2}{\partial\theta^2_{\vec{j}}}, \tag{7}$$

which describes the so-called quantum phase model (see e.g. [19,20]): in Eq.(7) $\theta_{\vec{j}}$ is the phase of the j-th condensates and

$$H_{XY} = -J \sum_{<\vec{i},\vec{j}>} \cos(\theta_{\vec{i}} - \theta_{\vec{j}}) \tag{8}$$

stands for the Hamiltonian of the classical XY model. When $J \gg U$ and at temperatures $T \gg U/k_B$, the pertinent partition function describing the thermodynamic behaviour of the BECs stored in an optical lattice may be computed using the classical XY model (8).

The close relationship of the Bose-Hubbard model (5) and the quantum phase model (7) is by now well known [21] and it has been widely used in the analysis of superconducting Josephson networks; since, in superconducting networks, N_0 is the average number of excess Cooper pairs at a given site, the requirement $N_0 \gg 1$ is of course satisfied and the condition $J/N_0^2 \ll U$ may also be easily realized for reasonable values of J. At variance, in bosonic lattices N_0 varies usually between ~ 1 and $\sim 10^3$ and the validity of the mapping between the Bose-Hubbard model and the quantum phase Hamiltonian is not always guaranteed; furthermore, in order to get the XY model (8) from the Bose-Hubbard model (5) U should be much smaller than J, but not vanishing, in order to satisfy to the condition $J/N_0^2 \ll U$. Of course the Bose-Hubbard model - for $U = 0$ - describes harmonic oscillators and thus cannot sustain any BKT transition; nevertheless, when $N_0 \gg 1$ and $J/N_0^2 \ll U \ll J$, the Bose-Hubbard Hamiltonian reduces in the XY model (8), which *do* display the BKT transition.

A simple estimate of the coefficients J and U may be obtained by approximating the Wannier functions in Eq.(4) with gaussians, whose widths are determined variationally. The details of the computation are reported in Appendix A. In Fig.1 we plot J/U as a function of V_0 for a $2D$ optical lattice; for comparison, we plot the same ratio for $1D$ and $3D$ optical lattices also. Since, in a mean-field approach, the Mott insulator-superfluid transition occurs at $T = 0$ approximately at $2zJ/U \sim 1$ [18,20] (z is the number of nearest-neighbours), from Fig.1 one sees that it is much easier to detect a quantum phase transition for the three-dimensional array (and indeed it has been recently detected [7]); no quantum phase transition has yet been reported in literature for $2D$ and $1D$ optical lattices, since a larger laser power V_0 is required for its observation.

For a $2D$ lattice with V_0 between 20 and $25E_R$ (and $N_0 \approx 170$ as in [6]), the conditions $J \gg U \gg J/N_0^2$ are rather well satisfied and the BKT critical temperature, $T_{BKT} \sim J/k_B$, is between 10 and $30nK$. Since the BKT transition for the XY model occurs at a temperature $T_{BKT} \sim J/k_B$, it should be possible to evidence the transition with measurements performed at different temperatures. Using a coarse-graining approach to determine the finite-temperature phase-boundary line of the Bose-Hubbard model [22], yields, in $2D$ and for $N_0 \gg 1$ and $J/U \gg 1$, a critical temperature $T_{BKT} \approx J/k_B$, in reasonable agreement with the XY estimates of T_{BKT}; in addition, in the chosen range of parameters, the condition $UN_0^2/J = UN_0/K \gg 1$, satisfies the finite-temperature stability criterion recently derived by Tsuchiya and Griffin [23].

We notice that the XY Hamiltonian, in the limits $N_0 \gg 1$ and $J \gg U \gg J/N_0^2$, can be also retrieved extending the Gross-Pitaevskii Hamiltonian to finite temperature $T \gg U/k_B$. Replacing the tight-binding ansatz $\Psi(\vec{r},t) = \sum_{\vec{j}} \psi_{\vec{j}}(t)\Phi_{\vec{j}}(\vec{r})$ (where $\psi_{\vec{j}}$ are classical fields and not operators) in the Gross-Pitaevskii Hamiltonian one gets the lattice Hamiltonian

$$H = -K \sum_{<\vec{i},\vec{j}>} (\psi_{\vec{i}}^* \psi_{\vec{j}} + c.c.) + \frac{U}{2} \sum_{\vec{j}} N_{\vec{j}}(N_{\vec{j}} - 1), \tag{9}$$

which is the classical version of the Bose-Hubbard model ($N_{\vec{j}} \equiv \mid \psi_{\vec{j}} \mid^2$). Writing $N_{\vec{j}} = N_0 + \delta N_{\vec{j}}$, one may neglect the quadratic terms [i.e. $(\delta N_{\vec{j}})^2$] in the hopping part of the Hamiltonian (9), which then reduces in the considered limit to H_{XY} (8).

Accurate Monte Carlo simulations yield - for the XY model - the BKT critical temperature $T_{BKT} = 0.898 J/k_B$ [24]. When $U \ll J$, a BKT transition still occurs at a slightly lower critical temperature $T_{BKT}(U)$. Intuitively speaking, when U increases, the superfluid region in the phase diagram decreases and, thus, one has $T_{BKT}(U) < T_{BKT}$ [20]. An estimate of the dependence of $T_{BKT}(U)$ on U obtained using a renormalization group approach has been reported in [25]: when $U \neq 0$, but still $U/J \ll 1$, the only effect of the interacting term amounts to renormalize J and to lower the BKT critical temperature [26]. For this reason in the following we shall present results from Monte Carlo simulations of the classical XY model only.

In numerical simulations of the finite XY lattice one defines the critical temperature as the temperature $T_C(L)$ at which the correlation length equals the size L of the square lattice [15]; of course, as $L \to \infty$, $T_C(L) \to T_{BKT}$. For $T = T_C(L)$, the BKT transition is signaled in a finite system by the fact that a suitably defined magnetization, defined by Eq.(11), drops to zero [15].

The emerging physical picture is the following: There are two relevant temperatures for the system, the temperature T_{BEC}, at which in each well there is a condensate, and the temperature T_{BKT} at which the condensates phases start to coherently point in the same direction. Of course, in order to have well defined condensates phases one should have $T_{BKT} < T_{BEC}$. The critical temperature T_{BEC} is given by $T_{BEC} \approx 0.94\hbar N_0^{1/3}\bar{\omega}/k_B$ where $\bar{\omega} = (\tilde{\omega}_r^2\omega_z)^{1/3}$ [27]. With the numerical values given in [6], T_{BEC} turns out to be $\gtrsim$ $500nK$ for $s \gtrsim 20$. When $T < T_{BEC}$, the atoms in the well $\vec{j}$ of the $2D$ optical lattice may be described by a macroscopic wavefunction $\psi_{\vec{j}}$. Furthermore, when the fluctuations around the average number of atoms per site $N_0 \gg 1$ are strongly suppressed, one may put, apart from the factor $\sqrt{N_0}$ constant across the array, $\psi_{\vec{j}} = e^{i\theta_{\vec{j}}}$. The temperature T_{BKT} is of order of J/k_B: with the experimental parameters of [6] and V_0 between 20 and $25E_R$, one has that T_{BKT} is between 10 and $30nK$, which is sensibly smaller than the condensation temperature T_{BEC} of the single well.

A similar scenario describes also the phases of planar arrays of superconducting Josephson junctions [19,20]: they exhibit a temperature T_{BCS} at which the metallic grains placed on the sites of the array become (separately) superconducting and the Cooper pairs may be described by macroscopic wavefunctions. At a temperature $T_{BKT} < T_{BCS}$, the array undergo a BKT transition and the system - as a whole - becomes superconducting.

III. OBSERVABLE SIGNATURE OF THE BKT TRANSITION

In this Section we shall evidence that the experimental signature of the BKT transition in bosonic planar lattices is obtained by measuring, as a function of the temperature, the central peak of the interference pattern obtained after turning off the confining potentials.

Firstly, we show that the peak of the momentum distribution at $\vec{k} = 0$ is the direct analog of the magnetization of a finite size $2D$ XY magnet. In fact, for the XY magnets, the spins can be written as $\vec{S}_{\vec{j}} = (\cos\theta_{\vec{j}}, \sin\theta_{\vec{j}})$ and the magnetization is defined as $M = (1/N) \cdot \langle \mid \sum_{\vec{j}} \vec{S}_{\vec{j}} \mid \rangle$ where $\langle \cdots \rangle$ stands for the thermal average; a spin-wave analysis at low temperatures yields $M = (2N)^{-k_B T/8\pi J}$ [15,14]. With discrete BECs at $T = 0$, all the phases $\theta_{\vec{j}}$ are equal at the equilibrium and the lattice Fourier transform of ψ_j,

$$\tilde{\psi}_{\vec{k}} = \frac{1}{N} \sum_{\vec{j}} \psi_{\vec{j}} \; e^{-i\vec{k}\cdot\vec{j}}, \tag{10}$$

exhibits a peak at $\vec{k} = 0$ ($\vec{k}$ is in the first Brillouin zone of the $2D$ square lattice); the magnetization is then

$$M = \langle \mid \tilde{\psi}_0 \mid \rangle. \tag{11}$$

The intuitive picture of the BKT transition is the following: at $T = 0$, all the spins point in the same direction. As one can see from Fig.2(A), a single free vortex modifies the phase distribution far away from the vortex core and, thus, the modulus square of its lattice Fourier transform $\mid \tilde{\psi}_{\vec{k}} \mid^2$ has a minimum at $\vec{k} = 0$. At variance, a vortex-antivortex pair [see Fig.2(B)] modifies the phase distribution only near the center of the pair (in this sense is a local *defect*) and its lattice Fourier transform has a maximum at $\vec{k} = 0$. Analytical expressions for the lattice Fourier transform $\tilde{\psi}_{\vec{k}}$ of a single vortex and a vortex-antivortex pair may be worked out in detail and are reported in the Appendix B.

Upon increasing the temperature, vortices are thermally induced. For $T < T_{BKT}$ only bound vortex pairs are present, and on average the spins continue to point in the same direction. When the condensates expand, a large peak (i.e., a magnetization) is observed in the central $\vec{k} = 0$ momentum component, as shown in Fig.2(C). Rising further the temperature, due to the increasing number of vortex pairs, the central peak density decreases. For $T \approx T_{BKT}$, the pairs start to unbind and free vortices begin to appear [see Fig.2(D)], determining a sharp decrease around T_{BKT} of the magnetization. At high temperatures, only free vortices are present, leading to a randomization of the phases and to a vanishing magnetization. In Fig.3 we plot the intensity of the central peak of the momentum distribution (normalized to the value at $T = 0$) in a 2D lattice as a function of the reduced temperature $k_B T/J$, evidencing the sharp decrease of the magnetization around the BKT critical temperature.

Let us now turn our attention to the interference patterns of the expanding condensates: after the bosonic system reaches the equilibrium, one may switch off both the harmonic trap and the optical lattice. At this time ($t = 0$) the momentum distribution $\tilde{\psi}(\vec{p}, t = 0)$ is given by the Fourier transform of $\psi(\vec{r}, t = 0) = \sum_{\vec{j}} \psi_{\vec{j}} \Phi_{\vec{j}}(\vec{r})$: one finds

$$\tilde{\psi}(\vec{p}, t = 0) = \tilde{\Phi}(\vec{p}) \tilde{\psi}_{\vec{k}}, \tag{12}$$

where $\tilde{\Phi}(\vec{p})$ is the Fourier transform of the $3D$ Wannier functions and $\hbar\vec{k} = (p_x, p_y)$ is the momentum projection on the first Brillouin zone of the $2D$ optical lattice. Using a gaussian for the Wannier functions, $\Phi(\vec{r}) \propto e^{-x^2/2\sigma_x^2} e^{-y^2/2\sigma_y^2} e^{-z^2/2\sigma_z^2}$ (with $\sigma_z \gg \sigma \equiv \sigma_x = \sigma_y$, since $\tilde{\omega}_r \gg \omega_z$), one has $\tilde{\Phi}(\vec{p}) = \chi(p_x)\chi(p_y)\chi(p_z) \propto e^{-\sigma^2(p_x^2+p_y^2)/2\hbar^2}$, where $\chi(p_x) \propto e^{-\sigma_x^2 p_x^2/2\hbar^2}$ and similarly for $\chi(p_y)$ and $\chi(p_z)$. Since for $s \gg 1$ $\sigma/d = 1/\pi s^{1/4}$, the momentum distribution exhibits well pronounced peaks in the centers of each Brillouin zone: these peaks have different heights and the central $\vec{k} = 0$ peak is the largest (see Figs.2 and 3 of [6]).

At $t = 0$ the amplitude of the $\vec{k} = 0$ peak of the momentum distribution is simply given by the thermal average of $\tilde{\psi}_0$. By measuring the $\vec{k} = 0$ peak (i.e., $\langle \mid \tilde{\psi}_0 \mid^2 \rangle$) at different temperatures, one obtains the results plotted in Fig.2. The figure has been obtained using a Monte Carlo simulation of the XY magnet for a 40×40 array: we find $k_B T_C \approx 1.07J$. In Fig.2 we also plot the low-temperature spin wave prediction [14] (solid line), as well as a fit, first used in [15], valid near T_C and derived form the renormalization group equations (dotted line). At times different from $t = 0$, the density profiles are well reproduced by the free expansion of the ideal gas: one obtains $\tilde{\psi}(\vec{p}, t) = \chi(p_z) e^{-i[(p_z+mgt)^3 - p_z^3]/6m^2 g\hbar} \tilde{\varphi}(p_x, p_y, t)$, i.e. a uniformly accelerating motion along z and a free motion in the $x - y$ plane, with $\tilde{\varphi}(p_x, p_y, t) = \chi(p_x)\chi(p_y)\tilde{\psi}_{\vec{k}} e^{-i(p_x^2+p_y^2)t/2\hbar m}$ giving the central and lateral peaks of the momentum distribution as a function of time for different temperatures.

An intense experimental work is now focusing on the Bose-Einstein condensation in two dimensions: at present a crossover to two-dimensional behaviour has been observed for Na [28] and Cs atoms [29]. Our analysis relies on two basic assumptions; namely, the validity of the tight-binding approximation for the Bose-Hubbard Hamiltonian and the requirement that the condensate in the optical lattice may be regarded as planar [30]. It is easy to see that the first assumption is satisfied if, at $T = 0$, $V_0 \gg \mu$ (where μ is the chemical potential), and, at finite temperature, $\hbar\tilde{\omega}_r \gtrsim k_B T$. The second assumption is much more restrictive since it requires freezing the transverse excitations; for this to happen one should require a condition on the transverse trapping frequency ω_z. Namely, one should have that, at $T = 0$, $\hbar\omega_z \gtrsim 8K$ and that, at finite temperature, $\hbar\omega_z \gtrsim k_B T$ (since $\omega_z \ll \tilde{\omega}_r$, the latter condition also implies that $\hbar\tilde{\omega}_r \gtrsim k_B T$). In [6] it is $V_0 = s \cdot k_B \cdot 0.15\mu K$ and, for $s \gtrsim 20$, the tight-binding conditions are satisfied since $10Hz \gtrsim 8K/2\pi\hbar$; furthermore, if $\omega_z = 2\pi \cdot 1kHz$, one may safely regard our finite temperature analysis to be valid at least up to $T \sim 50nK$. We notice that the experimental signature for the BKT transition for a continuous (i.e., without optical lattice) weakly interacting 2D Bose gas [31] is also given by the central peak of the atomic density of the expanding condensates.

IV. CONCLUDING REMARKS

Our paper analyzes the finite-temperature phase transitions in $2D$ lattices of BECs. Our study evidences the possibility that Bose-Einstein condensates loaded on a $2D$ optical lattice may exhibit - at finite temperature - a new coherent behaviour in which all the phases of the condensates located in each well of the lattice point in the same direction. The finite-temperature transition, which is due to the thermal atoms in each well, is mediated by vortex defects and may be experimentally detectable by looking at the interference patterns of the expanding condensates. Our analysis relies on the approximation that the effect of the shallow confining harmonic trap in the $x-y$ plane may be neglected: for a tight confinement, we expect that interesting mesoscopic effects will come to play, affecting the BKT transition.

We observe that for a $3D$ optical lattice (resulting form the potential $V_{opt}(\vec{r}) = V_0[\sin^2(kx) + \sin^2(ky) + \sin^2(kz)]$) with $N_0 \sim 100$, the system maps on the $3D$ XY model, which is the prototype of the universality class including the λ normal-superfluid transition in ${}^4He$ [32]. Also in this case, the central peak of the interference pattern tends to zero at the critical temperature, Fig.4. We recall, however, that the $3D$ transition is a simple order-disorder transition (whose critical temperature T_c is given in the thermodynamic limit by $2.202J/k_B$ [33]), and is not mediated by the creation of vortices-antivortices pairs as in the 2D case. A natural question arising from the comparison of Figs.3 and 4 is how to clearly characterize the two transitions: to answer, one may observe that the critical exponent β (defined by $M \propto (T_c - T)^\beta$) is $\beta \approx 0.23$ for the $2D$ XY universality class [15] and $\beta \approx 0.35$ for the $3D$ XY universality class [34].

In conclusion, our analysis strengthens - and extends at finite temperature - the striking and deep analogy of bosonic systems with superconducting Josephson junction arrays [1].

Acknowledgements: We thank Prof. E. Rastelli for stimulating discussions and for pointing our attention to Refs. [15]. P.S. and A.T. enjoyed very much the residence at the CRS-BEC of Trento, where this work was initiated. This work has been supported by MIUR through grant No. 2001028294 and by the DOE.

APPENDIX A: VARIATIONAL ESTIMATES OF THE COEFFICIENTS K AND U

In this Appendix we derive a variational estimate of the coefficients K and U entering the Bose-Hubbard Hamiltonian (5). The tunneling rate K and the coefficient of the nonlinear term U are given by

$$K = -\int d\vec{r} \left[\frac{\hbar^2}{2m} \vec{\nabla}\Phi_{\vec{i}} \cdot \vec{\nabla}\Phi_{\vec{j}} + \Phi_{\vec{i}} V_{ext} \Phi_{\vec{j}} \right] \tag{A1}$$

and

$$U = g_0 \int d\vec{r}\, \Phi_{\vec{j}}^4, \tag{A2}$$

where $g_0 = 4\pi\hbar^2 a/m$ and $\Phi_{\vec{j}}(\vec{r})$ is the Wannier wavefunction localized at the $\vec{j}$-th well and normalized to 1.

For a $2D$ optical lattice in the $x-y$ plane one has $V_{ext} = V_{opt} + V_m$, where the optical potential is $V_{opt} = V_0[\sin^2(kx) + \sin^2(ky)]$ and the magnetic potential is $V_m = \frac{m}{2}[\omega_r^2(x^2 +$

$y^2) + \omega_z^2 z^2]$. Typical values of the parameters relevant for experiments [6] are $\omega_r, \omega_z \sim 2\pi \cdot 10 - 100\,Hz$, $\lambda = 852\,nm$, for a total number of sites ~ 3000 and an average number of particles per site ~ 170. The condition $\omega_z \gg \omega_r$ should be imposed in order to have a $2D$ system. To get a variational estimate for K and U we assume that the Wannier wavefunction localized at the j-th well is given by

$$\Phi_{\vec{j}}(\vec{r}) = C e^{-(x-x_j)^2/2\sigma_x^2} e^{-(y-y_j)^2/2\sigma_y^2} e^{-(z-z_j)^2/2\sigma_z^2}. \tag{A3}$$

In Eq.(A3) the parameters σ_x, σ_y, and σ_z have to be determined variationally determined, C is a normalization constant given by $C = (\pi^{3/2}\sigma^2\sigma_z)^{-1/2}$ and (x_j, y_j, z_j) are the coordinates of the center of the j-th well. Due to the symmetry of the external potential one has to set $\sigma_x = \sigma_y \equiv \sigma$: furthermore, since $\tilde{\omega}_r \gg \omega_r, \omega_z$, one has $\sigma_z \gg \sigma$. To fix σ and σ_z one recalls that the Gross-Pitaevskii energy is [27]

$$\mathcal{E}[\Psi] = \int d\vec{r} \left[\frac{\hbar^2}{2m} (\vec{\nabla}\Psi)^2 + V_{ext} \mid \Psi \mid^2 + \frac{g_0}{2} \mid \Psi \mid^4 \right]. \tag{A4}$$

In the tight-binding approximation, $\Psi(\vec{r}, t) = \sum_j \psi_j(t)\Phi_j(\vec{r})$, one finds that the energy contribution E_i of the i-th well to the total energy (A4) is $E_i \approx \int d\vec{r} [\, \mid \psi_i \mid^2 \frac{\hbar^2}{2m} (\vec{\nabla}\Phi_i)^2 + V_{ext} \mid \psi_i \mid^2 \Phi_i^2 + \frac{g_0}{2} \mid \psi_i \mid^4 \Phi_i^4]$, and, since $\mid \psi_i \mid^2 \approx N_0$, N_0 being the average value of particle per site, one gets

$$E_i \approx \int d\vec{r} \left[N_0 \frac{\hbar^2}{2m} (\vec{\nabla}\Phi_i)^2 + N_0 V_{ext} \Phi_i^2 + \frac{g_0}{2} N_0^2 \Phi_i^4 \right]. \tag{A5}$$

Substituting (A3) in (A5), one gets the following approximate expression for the energy in the i-th well

$$\frac{E_i}{N_0} \approx \frac{\hbar^2}{2m} \left(\frac{1}{2\sigma_z^2} + \frac{1}{\sigma^2} \right) + \frac{m}{2} \left(\omega_r^2 \sigma^2 + \omega_z^2 \frac{\sigma_z^2}{2} \right) + V_0 k^2 \sigma^2 + \frac{g_0 N_0}{2(2\pi)^{3/2} \sigma^2 \sigma_z}. \tag{A6}$$

The optimal values of σ and σ_z are determined requiring that $\partial E_i / \partial \sigma = 0$ and $\partial E_i / \partial \sigma_z = 0$. It should be stressed that being σ the variational width in the directions x and y, it should be less than $\lambda/2$, the distance between minima of the periodic potential. We notice also that for realistic values of the parameters, the variational width σ in the x and y directions has a very weak dependence on the mean field term (and therefore to the number of particles in each site): in fact, putting $\sigma \sim 0.2\mu m$ and $\sigma_z \sim 5\mu m$, one finds $\hbar^2/2m\sigma^2 \sim 10^{-23}erg \gg g_0 N_0/2(2\pi)^{3/2}\sigma^2\sigma_z \sim 10^{-29}erg$, one sees that the last term in Eq.(A6) contributes very little to the determination of σ. Since $V_0 k^2 \gg m\omega_r^2/2$, from Eq.(A6) one then finds that the dependence of E_i on σ is given by $E_i(\sigma) \approx N_0(\hbar^2/2m\sigma^2 + V_0 k^2\sigma^2)$: from $\partial E_i/\partial\sigma = 0$ one obtains $\sigma^4 = \hbar^2/2mk^2V_0$, which can be cast in the form $\sigma = \lambda\,\chi$, with

$$\chi = \frac{1}{2\pi s^{1/4}} \tag{A7}$$

and $s = V_0/E_R$.

We are now in position to have an estimate for K and U: by using the ansatz (A3) in Eqs.(A1)-(A2) we get

$$\frac{K}{E_R} = \frac{1}{4\pi^2\chi^4}\left(\frac{1}{16} - \chi^2\right) e^{-1/16\chi^2} - s e^{-1/16\chi^2} \tag{A8}$$

and

$$\frac{U}{E_R} = \frac{2mg_0}{(2\pi)^{7/2}\hbar^2\sigma_z\chi^2}. \tag{A9}$$

The variational procedure used works well also for $1D$ and $3D$ optical lattices: in a $1D$ optical lattice in the x direction one has $V_{ext} = V_{opt} + V_m$, where $V_{opt} = V_0 \sin^2(kx)$ and $V_m = \frac{m}{2}[\omega_x^2 x^2 + \omega_\perp^2(y^2+z^2)]$. Typical values of the parameters relevant for experiments [2] are $\omega_x \approx 2\pi\cdot 10\,Hz$, $\omega_\perp \approx 2\pi \cdot 100\,Hz$, $\lambda = 795\,nm$, for a total number of sites ~ 100 and an average number of particles per site ~ 1000. The variational ansatz is still given by Eq.(A3), but now $\sigma_y = \sigma_z \equiv \sigma_\perp$ and $\sigma_x \equiv \sigma$ is the variational width in the laser direction. Proceeding as before, one obtains that $\sigma = \lambda\,\chi$, with χ still given by Eq.(A7). The tunneling rate K is given by

$$\frac{K}{E_R} = \frac{1}{4\pi^2\chi^4}\left(\frac{1}{16} - \frac{\chi^2}{2}\right) e^{-1/16\chi^2} - \frac{s}{2}\,(1 + e^{-4\pi^2\chi^2})\, e^{-1/16\chi^2}, \tag{A10}$$

and the nonlinear coefficient U reads $U/E_R = 2m\lambda g_0/(2\pi)^{7/2}\hbar^2\sigma_\perp^2\chi$ where χ is given by Eq.(A7).

For a $3D$ optical lattice one has $V_{ext} = V_{opt} + V_m$, where $V_{opt} = V_0[\sin^2(kx) + \sin^2(ky) + \sin^2(kz)]$ and $V_m = \frac{m}{2}\omega(x^2+y^2+z^2)$. Typical experimental values from [7] are $\omega \approx 2\pi\cdot 50\,Hz$, $\lambda = 852\,nm$, for a total number of sites $\sim 10^5$ and an average number of particles per site ~ 1. The variational ansatz is still given by Eq.(A3), but now $\sigma_x = \sigma_y = \sigma_z \equiv \sigma$. One obtains that $\sigma = \lambda\,\chi$, with χ given as before by Eq.(A7). The tunneling rate K is given by

$$\frac{K}{E_R} = \frac{1}{4\pi^2\chi^4}\left(\frac{1}{16} - \frac{3\chi^2}{2}\right)e^{-1/16\chi^2} - s\left(\frac{3}{2} - \frac{1}{2}e^{-4\pi^2\chi^2}\right)e^{-1/16\chi^2}, \tag{A11}$$

and the nonlinear coefficient U reads $U/E_R = 2mg_0/(2\pi)^{7/2}\hbar^2\lambda\chi^3$.

We observe that the tunneling rates K for $1D$, $2D$ and $3D$ optical lattices, given respectively by Eqs.(A10), (A8) and (A11), can be compactly written as

$$\frac{K}{E_R} = \frac{1}{4\pi^2\chi^4}\left(\frac{1}{16} - \frac{(j+1)\chi^2}{2}\right)e^{-1/16\chi^2} - s\left(\frac{j+1}{2} - \frac{j-1}{2}e^{-4\pi^2\chi^2}\right)e^{-1/16\chi^2}, \tag{A12}$$

where $j = D - 1$.

APPENDIX B: FOURIER TRANSFORM OF A VORTEX ON A LATTICE

In this Appendix we report the analytical computation of the lattice Fourier transform $\tilde{\psi}_{\vec{k}}$ of single vortex on a lattice described by $\psi_{\vec{j}} = \exp(i\theta_{\vec{j}})$; namely, one should compute

$$\tilde{\psi}_{\vec{k}} = \frac{1}{N}\sum_{\vec{j}} \psi_{\vec{j}}\; e^{-i\vec{k}\cdot\vec{j}} = \frac{1}{N}\sum_{\vec{j}} e^{-i\vec{k}\cdot\vec{j}+i\theta_{\vec{j}}}. \tag{B1}$$

In Eq.(B1), $\vec{j} = (j_x, j_y)$ denotes the sites of a square lattice (having N sites) and $\vec{k} = (k_x, k_y)$ the (quasi)momentum, with k_x and k_y valued between $-\pi$ and π. The relationship between the lattice Fourier transform (B1) and the momentum distribution $\tilde{\psi}(\vec{p})$ in real space is provided by Eq.(12).

To simplify matters, in this Appendix we set the origin O of the coordinates in the center of the central plaquette: setting to 1 the lattice length, the lattice sites are labeled by $\vec{j} = (j_1/2, j_2/2)$ with j_1 and j_2 positive and negative *odd* integer numbers.

The phase distribution of a vortex is depicted in Fig.2(A) and is such that $\theta_{\vec{j}}$ equals the polar angle ϕ with respect to the origin O (e.g., at the site $(1/2, 1/2)$ $\theta_{\vec{j}}$ equals $\pi/4$, at the site $(3/2, 1/2)$ is $\arctan(1/3)$, and so on; an antivortex would be characterized by $-\phi$). For future convenience, we shall label the site $(j_1 + 1/2, j_2 + 1/2)$ with the index $\ell = (\mid j_1 \mid + \mid j_2 \mid)/2$: as a consequence, the four sites $(1/2, 1/2)$, $(1/2, -1/2)$, $(-1/2, 1/2)$, and $(1/2, 1/2)$ of the central plaquette will be associated to $\ell = 1$; the eight sites $(3/2, 1/2)$, $(1/2, 3/2)$, $\cdots$, $(-3/2, 1/2)$ will be associated to $\ell = 2$. In other words, the sites with index ℓ have chemical distance $\ell - 1$ from the four sites of the central plaquette. Of course, the number of sites with index ℓ is 4ℓ. If, for simplicity, one considers only sites with ℓ going from 1 to a maximum value $\mathcal{L}$, then the total number of sites is

$$N(\mathcal{L}) = \sum_{\ell=1}^{\mathcal{L}} 4\ell = 2\mathcal{L}(\mathcal{L}+1). \tag{B2}$$

To evaluate the lattice Fourier transform (B1), one may conveniently separate the sum $\sum_{\vec{j}} e^{-i\vec{k}\cdot\vec{j}+i\theta_{\vec{j}}}$ in $\mathcal{L}$ sums over sites having the same index ℓ; for instance, for the four sites $(1/2, 1/2)$, $(1/2, -1/2)$, $(-1/2, 1/2)$, and $(1/2, 1/2)$ of the central plaquette, one gets

$$\sum_{\vec{j}(1)} e^{-i\vec{k}\cdot\vec{j}+i\theta_{\vec{j}}} = 4\left[\sin\phi_1^{(1)} \cos\frac{k_x}{2} \sin\frac{k_y}{2} - i\cos\phi_1^{(1)} \sin\frac{k_x}{2} \cos\frac{k_y}{2}\right] \tag{B3}$$

where $\phi_1^{(1)} = \pi/4$ and the sum is restricted only to the sites having $\ell = 1$. A straightforward generalization of Eq.(B3) shows that for the sum on the 4ℓ sites having a fixed ℓ one has

$$\tilde{\psi}_{\vec{k}}^{(\ell)} \equiv \sum_{\vec{j}(\ell)} e^{-i\vec{k}\cdot\vec{j}+i\theta_{\vec{j}}} = 4\sum_{m=1}^{\ell}\left[\sin\phi_m^{(\ell)} \cos\frac{(2n-2m+1)k_x}{2} \sin\frac{(2m-1)k_y}{2} + \right.$$
$$\left. -i\cos\phi_m^{(\ell)} \sin\frac{(2n-2m+1)k_x}{2} \cos\frac{(2m-1)k_y}{2}\right] \tag{B4}$$

where

$$\phi_m^{(\ell)} = \arctan\left[\frac{2m-1}{2n-2m+1}\right] \tag{B5}$$

is an angle taking values between 0 and $\pi/2$.

By using Eq.(B4), the lattice Fourier transform (B1) may be compactly written as

$$\tilde{\psi}_{\vec{k}} = \frac{1}{N(\mathcal{L})} \sum_{\ell=1}^{\mathcal{L}} \tilde{\psi}_{\vec{k}}^{(\ell)}. \tag{B6}$$

If in Eq.(B6) one puts $k_y = 0$, one gets

$$\tilde{\psi}_{\vec{k}} = \frac{-4i}{N(\mathcal{L})} \sum_{\ell=1}^{\mathcal{L}} \sum_{m=1}^{\ell} \cos\phi_m^{(\ell)} \sin\frac{(2n-2m+1)k_x}{2}; \tag{B7}$$

by introducing the index $\tilde{m} = \ell - m$ and rearranging conveniently the partial sums in Eq.(B7) one obtains

$$\tilde{\psi}_{\vec{k}} = \sum_{\tilde{m}=0}^{\mathcal{L}-1} a_{\tilde{m}} \sin\frac{(2\tilde{m}+1)k_x}{2} \tag{B8}$$

with

$$a_{\tilde{m}} = \frac{-4i}{N(\mathcal{L})} \sum_{n=\tilde{m}+1}^{\mathcal{L}} \frac{2\tilde{m}+1}{\sqrt{(2\tilde{m}+1)^2 + (2n-2\tilde{m}-1)^2}}.$$

Eq.(B8) clearly shows that for $k_x = 0$ one has $\tilde{\psi}_0 = 0$: of course, with a single vortex, the magnetization (11) is zero; furthermore, in the thermodynamic limit $\mathcal{L} \to \infty$, $a_{\tilde{m}} \to 0$, in agreement the Mermin-Wagner theorem. We observe Eq.(B6) may be easily applied to the analysis of the lattice Fourier transform of a vortex-antivortex pair.

REFERENCES

[1] B. P. Anderson and M. A. Kasevich, Science **282**, 1686 (1998).

[2] F. S. Cataliotti, S. Burger, C. Fort, P. Maddaloni, F. Minardi, A. Trombettoni, A. Smerzi, and M. Inguscio, Science **293**, 843 (2001).

[3] O. Morsch, J. H. Müller, M. Cristiani, D. Ciampini, and E. Arimondo Phys. Rev. Lett. **87**, 140402 (2001).

[4] W. K. Hensinger *et al.*, Nature **412**, 52 (2001).

[5] B. Eiermann, P. Treutlein, T. Anker, M. Albiez, M. Taglieber, K.-P. Marzlin, and M. K. Oberthaler Phys. Rev. Lett. **91**, 060402 (2003).

[6] M. Greiner, I. Bloch, O. Mandel, T. W. Hänsch, and T. Esslinger, Phys. Rev. Lett. **87**, 160405 (2001).

[7] M. Greiner, O. Mandel, T. Esslinger, T. W. Hänsch, and I. Bloch, Nature **415**, 39 (2002).

[8] M. R. Beasley, J. E. Mooij, and T. P. Orlando, Phys. Rev. Lett. **42**, 1165 (1979).

[9] D. J. Resnick *et al.*, Phys. Rev. Lett. **47**, 1542 (1981).

[10] D. R. Nelson, in *Phase Transitions and Critical Phenomena*, vol. 7, eds. C. Domb and J. L. Lebowitz (New York, Academic Press, 1983) and references therein.

[11] P. Minnaghen, Rev. Mod. Phys. **59**, 1001 (1987).

[12] L. P. Kadanoff, *Statistical Physics: Statics, Dynamics and Renormalization* (Singapore, World Scientific, 2000), Chapt.s 16-17 and reprints therein.

[13] D. J. Bishop and J. D. Reppy, Phys. Rev. Lett. **40**, 1727 (1978).

[14] V. L. Berezinskii and A. Ya. Blank, Sov. Phys. JETP **37**, 369 (1973).

[15] S. T. Bramwell and P. C. W. Holdsworth, J. Phys.: Condensed Matter **5**, L53 (1993);

Phys. Rev. B **49**, 8811 (1994).

[16] P. Pedri and L. Santos, Phys. Rev. Lett. **91**, 110401 (2003).

[17] D. Jaksch, C. Bruder, J. I. Cirac, C. W. Gardiner, and P. Zoller, Phys. Rev. Lett. **81**, 3108 (1998).

[18] M. P. A. Fisher, P. B. Weichman, G. Grinstein, and D. S. Fisher, Phys. Rev. B **40**, 546 (1989).

[19] E. Simànek, *Inhomogeneous Superconductors*, Oxford University Press, New York, 1994.

[20] R. Fazio and H. van der Zant, Phys. Rep. **355**, 235 (2001).

[21] M. P. A. Fisher and G. Grinstein, Phys. Rev. Lett. **60**, 208 (1988).

[22] A. P. Kampf and G. T. Zimanyi, Phys. Rev. B **47**, 279 (1993).

[23] S. Tsuchiya and A. Griffin, cond-mat/0311321.

[24] R. Gupta, J. DeLapp, G. G. Batrouni, G. C. Fox, C. F. Baillie, and J. Apostolakis, Phys. Rev. Lett. **61**, 1996 (1988).

[25] A. Smerzi, P. Sodano, and A. Trombettoni, J. Phys. B **37**, S265 (2004).

[26] C. Rojas and J. V. José, Phys. Rev. B **54**, 12361 (1996).

[27] L. P. Pitaevskii and S. Stringari, *Bose-Einstein Condensation* (Oxford University Press, Oxford, 2003).

[28] A. Görlitz *et al.*, Phys. Rev. Lett. **87**, 130402 (2001).

[29] M. Hammes, D. Rychtarik, B. Engeser, H.-C. Nágerl, and R. Grimm, Phys. Rev. Lett. **90**, 173001 (2001).

[30] D. S. Petrov, M. Holzmann, and G. V. Shlyapnikov, Phys. Rev. Lett. **84**, 2551 (2000).

[31] N. Prokofév, O. Ruebenacker, and B. Svistunov, Phys. Rev. Lett. **87**, 270402 (2001).

[32] D. R Tilley and J. Tilley, *Superfluidity and Superconductivity* (Bristol, Adam Hilger, 1990).

[33] A. P. Gottlob and M. Hasenbusch, Physica A **201**, 593 (1993).

[34] M. Campostrini, M. Hasenbusch, A. Pelissetto, P. Rossi, and E. Vicari, Phys. Rev. **B 63**, 214503 (2003).

FIGURES

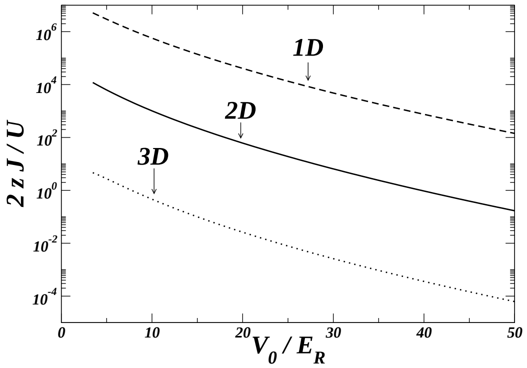

FIG. 1. J/U as a function of V_0/E_R for $1D$, $2D$ and $3D$ optical lattices (z is the number of nearest neighbours, which is respectively 2, 4, and 6). The experimental values are taken, respectively, from [2], [6], and [7], with an average number of ^{87}Rb atoms $N_0 = 1000$ ($1D$), 170 ($2D$) and 1 ($3D$).

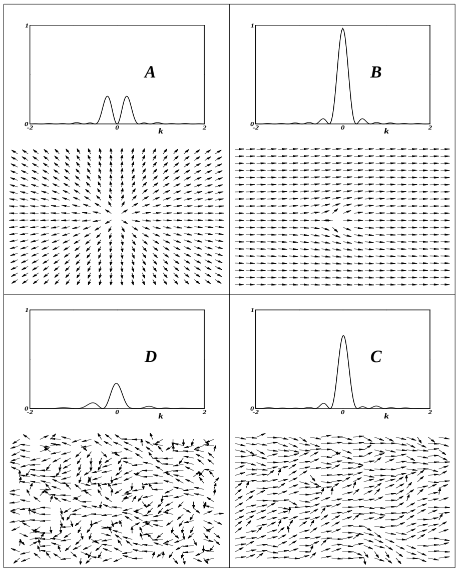

FIG. 2. Lattice Fourier transform $\mid \tilde{\psi}_{\vec{k}} \mid^2$ (for $k_y = 0$) with: (A) a single lattice vortex; (B) a lattice vortex-antivortex pair; (C) $T = 0.5J/k_B$; (D) $T = 1.1J/k_B$. Figures (C) and (D) are Monte Carlo snapshots after reaching equilibrium. The lattice is 20×20.

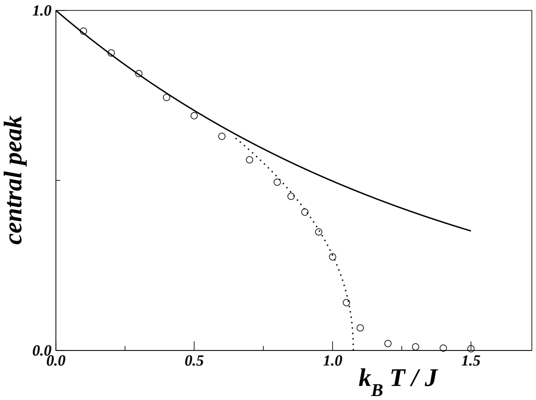

FIG. 3. Intensity of the central peak of the momentum distribution (normalized to the value at $T = 0$) as a function of the reduced temperature $t = k_B T/J$ in a 2D lattice. Empty circles: Monte Carlo simulations; solid line: low-temperature spin wave prediction; dotted line: fit near $T_C \approx 1.07 J/k_B$ as in [15] (in this figure $L = 40$).

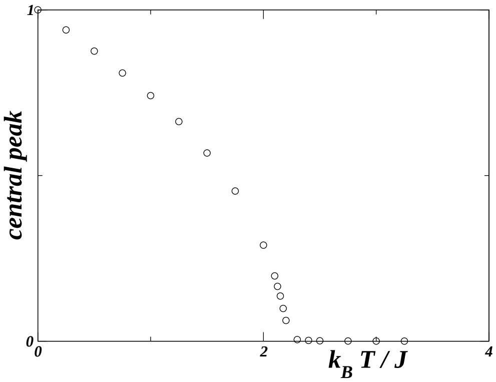

FIG. 4. Monte Carlo results for the intensity of the central peak of the momentum distribution (normalized to the value at $T = 0$) as a function of the reduced temperature $t = k_B T/J$ in a 3D lattice (with 20^3 sites).